https://doi.org/10.5194/acp-2019-1027
Preprint. Discussion started: 19 November 2019

Atmospheric Chemistry and Physics Discussions

Seasonal source variability of carbonaceous aerosols at the Rwanda climate Observatory

August Andersson[1], Elena N Kirillova[1,2], Stefano Decesari[2], Langley DeWitt[3], Jimmy Gasore[3,4,5], Katherine E Potter[3], Ronald G Prinn[3], Maheswar Rupakheti[6], Jean de Dieu Ndikubwimana[4], Julius Nkusi[4], Bonfils Safari[5].

[1] Department of Environmental Science and Analytical Chemistry (ACES) and the Bolin Centre for Climate Research, Stockholm University, SE-10691 Stockholm, Sweden

[2] Institute of Atmospheric Sciences and Climate-ISAC, National Research Council of Italy, Bologna, Italy

[3] Center for Global Change Science, Massachusetts Institute of Technology, Cambridge, MA, USA

[4] Climate Secretariat, Ministry of Education, Kigali, Rwanda

[5] Physics Department, School of Physics, College of Science and Technology, University of Rwanda, Kigali, Rwanda

[6] Institute for Advanced Sustainability Studies (IASS), Potsdam, Germany

Correspondence: August Andersson (august.andersson@aces.su.se)

https://doi.org/10.5194/acp-2019-1027
Preprint. Discussion started: 19 November 2019

Atmospheric Chemistry and Physics Discussions

Abstract

Sub-Saharan Africa (SSA) is a global hotspot for aerosol emissions, affecting regional environmental sustainability. In this paper we use atmospheric observations to address one of the major uncertainties of the, e.g., climate and health impact of SSA aerosols: the quantitative contributions from different emissions sources. Ambient fine fraction aerosol ($PM_{2.5}$) were collected on filters at the high altitude (2590 m.a.s.l.) Rwanda Climate Observatory (RCO), an SSA background site, during dry and wet seasons in 2014 and 2015. The concentrations of both carbonaceous aerosols and inorganic ions show a strong seasonal cycle, with highly elevated concentrations during the dry season. Source marker ratios, including carbon isotopes, show that the wet and dry seasons have distinct aerosol compositions. The dry season is characterized by elevated amounts of biomass burning products, approaching ~ 95% for carbonaceous aerosols. An isotopic mass-balance estimate shows that the amount of the carbonaceous aerosols stemming from savanna fires may increase from ~ 0.6 $\mu g/m^3$ in the wet season up to ~10$\mu g/m^3$ during the dry season. Taken together, we here quantitatively show that savanna fire is the key modulator of the seasonal aerosol composition variability at the RCO, an SSA background site.

https://doi.org/10.5194/acp-2019-1027
Preprint. Discussion started: 19 November 2019

1. Introduction

Sub-Saharan Africa (SSA) currently face major challenges for sustainable development, including industrial development, agriculture, fresh water supply, climate change, energy resources and air pollution (IPCC 2014; UNDP, 2018). Either directly, or indirectly, these challenges have linkage to aerosol emissions. Aerosols offset the ongoing regional climate warming in SSA, shift monsoon and precipitation pattern, are linked to both manmade (e.g., industry, traffic and agriculture) and ecosystem emissions, and are detrimental for air quality (IPCC 2013; WHO 2016). Ambient air pollution in SSA is estimated to cause 563.000 premature deaths annually, making it one of the main causes for mortality in the region (Bauer et al., 2019). However, the level of scientific understanding of the sources, properties and impacts of aerosols is not in parity with the multi-faceted societal impact. Central to this offset is the complex aerosol lifecycle, where emissions, transformations and sinks all are associated with large uncertainties, in particular given the vast physical and chemical complexity of these colloids. A major limiting factor in improving our understanding of these effects in the SSA are the limited number of in situ observations (Williams, 2007; Cais et al., 2011; Kulmala, 2018; López-Ballesteros et al., 2018).

A major source of aerosol emissions in SSA are dry season regional fires – clearly visible from space (Fig. 1). These may either be formed naturally, e.g., lightning strikes, but are mainly lit by humans (Bird and Cali, 1998; Archibald et al., 2012). There is evidence that slash-and-burn agriculture in SSA has been a common practice for thousands of years. This long-term anthropogenic perturbation is a significant modulator of the current ecosystem structure. A number of previous studies have been specifically focused on characterizing emissions of aerosols and gases from African fires, e.g., the Southern African Regional Science Initiative Project (SAFARI 2000), conducted between 1999 to 2001 (Swap et al., 2003). Ground- and airborne chemical characterization from this and other campaigns suggest a rather distinct chemical composition (Table 1).

Carbonaceous aerosols, often quantified as total carbon (TC), are generally divided into two main components: black carbon (BC; here we use elemental carbon (EC) to quantify the amounts of BC) and organic carbon (OC). Although overlapping to some extent, these two pools generally have quite different atmospheric lifecycles and environmental effects. Formed from incomplete combustion, sunlight-absorbing BC contributes to regional warming and is a particularly health

https://doi.org/10.5194/acp-2019-1027
Preprint. Discussion started: 19 November 2019

detrimental component in air pollution (WHO 2012; WMO/UNEP 2011; IPCC 2013; Bond et al., 2013). BC is chemically inert to atmospheric reactions, and thus the lifetime is mainly determined by deposition. OC is also emitted from incomplete combustion (with different emission factors) but is also emitted from non-combustion sources and is also formed in the air through secondary processes. OC is thought to have an overall cooling effect on the climate. Being more chemically reactive, the OC pool to some extent has a more complex atmospheric lifetime, with continuous heterogenous chemistry, rendering the lifetime dependent on both precipitation and chemical transformations. Emissions from SSA fires are expected to contribute to a large part of the total TC atmospheric burden.

In general, the actual environmental impact of TC on SSA is still poorly constrained. Bottom-up emissions projections suggests that the TC emissions from SSA are expected to increase rapidly during the coming decades, perhaps reaching 50% of the global OC burden by 2030 (Liousse et al., 2014). To quantify and evaluate such model predictions, as well as to characterize the overall aerosol composition, it is valuable to conduct measurements at regional background sites. Dual carbon isotope characterization ($\Delta^{14}C$ and $\delta^{13}C$) of TC at background sites in South and East Asia and the Arctic has been shown to be a valuable tool for quantitatively constraining the emissions from different sources (Gustafsson et al., 2009; Andersson et al., 2015; Sheesley et al., 2012; Kirillova et al., 2014; Winiger et al., 2019).

In this paper we present dual carbon isotope constraints of TC, along with chemical characterization of inorganic ions and different carbonaceous pools, from a study conducted at the Rwanda Climate Observatory (RCO), during October 2014 to September 2015. A key objective of the study was to estimate the relative contributions from major TC source categories at this regionally representative site in the SSA. In particular, we investigate the source variability associated with the seasonal variations between prevailing wet and dry monsoon periods in the region and the contributions from savanna fires.

2. Methods and Materials

2.1 Filter sampling

https://doi.org/10.5194/acp-2019-1027
Preprint. Discussion started: 19 November 2019

The sampling site, the Rwanda Climate Observatory (RCO), is located on the top of Mt. Mugogo, in the western mountainous Rwanda. (1.586° S, 29.566° E, 2590 m above sea level, 5 m above ground). The station was established as a collaboration between the Massachusetts Institute of Technology (MIT, USA) and the Rwandan Government in 2013. The station is described in more detail by DeWitt et al. (2019). The station is an Advanced Global Atmospheric Gases Experiment (AGAGE) network site (for full list of instruments see http://agage.mit.edu).

Quartz filter samples (Millpores, 150 mm diam) were collected with a high-volume sampler (DH-77, Digitel Inc. Switzerland) operating at $30 m^3 h^{-1}$ using a $PM_{2.5}$ inlet. Night-time only (1AM to 6AM) sampling was conducted to minimize the effects of local emissions and day-time local atmospheric chemistry and to increase likelihood to capture the regional, free troposphere, signals. This strategy is supported by high temporal investigations of the diurnal cycle of, e.g., BC (DeWitt et al., 2019). The filter-samples were pre-combusted together with aluminum foil envelopes (400ºC for 5h), and were treated with special attention to minimize contamination. The filter samples were subsequently shipped to Stockholm University for chemical/isotopic analysis. The samples were stored in freezers both on site and at Stockholm University. Field blanks were collected on a monthly basis. The present campaign covers the period October 2014 to September 2015. However, the period December 2014 to April 2015 is missing due to a lightning strike which damaged the instrument. Thus, this study presents results from analysis of filter samples (in total 25) collected for the periods that cover the beginning of the 2014 fall rainy season (Oct-Nov), the end of the spring 2015 rainy season (April – May) and the dry 2015 summer season (June – September). We jointly refer the October-November 2014 and the April-May 2015 periods as the wet periods.

2.2 Concentrations analysis

The concentrations of elemental carbon (EC – mass-based tracer for black carbon) and organic carbon (OC) were determined using a Sunset Inc. thermal-optical instrument using the NIOSH 4050 protocol (Birch and Cary, 1996; Table S1). Pre-treatment using acid fumigation with 1M HCl ensured efficient removal of carbonates. A glucose solution was used to calibrate the FID-response of the instrument, and the long-term performance of the instrument was checked through running of National Institute of Standards and Technology (NIST) Standard Reference Materials (SRM) standards. All the concentrations were blank corrected and the field blank input was on

https://doi.org/10.5194/acp-2019-1027
Preprint. Discussion started: 19 November 2019

average 2% for OC and 0% for EC. The average relative standard deviation of the triplicate analysis was 5% for OC, 7% for EC.

Water-soluble organic carbon (WSOC) was extracted from filter sub-samples in ultra-pure Milli-Q water through 1.5 hour shaking. The extracts were filtered using 0.45 µm cutoff PTFE syringe filters (Minisart-SRP 10, Sartorius Stedim biotech, Germany). The concentration of WSOC was quantified in the filtered solutions as a difference between total water-soluble carbon and water-soluble inorganic carbon using a high temperature catalytic oxidation instrument TOC-5000A (Shimadzu, Japan). The samples were neither acidified nor purged, to avoid the loss of volatile organic compounds. The accuracy of the measurement ranges from 7% for 1 $mg \cdot L^{-1}$ of carbon solution to 3% for concentrations higher than 2 $mg \cdot L^{-1}$ of carbon. All the measurements were blank corrected. WSOC field blanks corresponded to an average 0.5%. The average relative standard deviation of the triplicate analysis was 10%.

The concentrations of water-soluble inorganic anions were determined by ion chromatography using a Dionex ICS-2000 system. Anions were separated using an IonPac AG11 2x50 mm Dionex guard column, IonPac AS11 2x250 mm Dionex separation column and ASRS 300 self-regenerating suppressor. A solution of KOH was used as eluent. Cations were separated using an IonPac CG16 3x50 mm Dionex guard column, IonPac CS11 3x250 mm Dionex separation column and CSRS 300 self-regenerating suppressor. The analysis of cations was performed using 30 mM solution of MSA as eluent. Field blanks constituted on average 3% of NO^{3-}, 2% of SO_4^{2-} and 1% of NH_4^+ and K^+ ion concentrations. The triplicate analysis showed the average relative standard deviation of 2% for NO^{3-} and K^+, 5% for SO_4^{2-} and 6% for NH_4^+.

2.3 Isotope analysis

Approximately every second sample (n = 12) were selected for carbon isotope ($\Delta^{14}C$ and $\delta^{13}C$) analysis of total carbon (TC = OC + EC; Table S1). The filter samples were combusted using the Sunset analyzer (total carbon protocol) and the evolved CO_2 was collected in glass vials using a liquid nitrogen cryo-trap (e.g., Andersson et al., 2015). The vials were subsequently shipped to the National Ocean Sciences Accelerator Mass Spectrometry (NOSAMS) facility at the Woods Hole Oceanographic Institute for analysis of the dual carbon isotope signatures. The $\Delta^{14}C$-signature was

https://doi.org/10.5194/acp-2019-1027
Preprint. Discussion started: 19 November 2019

measured using accelerator mass spectrometry (AMS), while the δ^{13}C-signature was measured using an Isotope Ratio Mass Spectrometer (IRMS).

2.4 Source Apportionment

The Δ^{14}C-signature allows the differentiation between the relative contributions of biogenic/biomass burning and fossil sources. The fraction biogenic/biomass burning (f_{bio}) may be calculated using isotopic mass-balance (f_{fossil} = 1- f_{bio}):

$$\Delta^{14}C_{sample} = f_{bio} \cdot \Delta^{14}C_{bio} + (1 - f_{bio}) \cdot \Delta^{14}C_{fossil} \quad (1)$$

The fossil endmember is -1000‰, as it is completely depleted in ^{14}C. The biomass endmember is more complex. For annual plants it is fairly straight-forward: the biomass Δ^{14}C-signature equals the Δ^{14}C value of CO_2 for that year (~ +20‰ for 2014/15, Graven, 2015; Turnbull et al., 2017). For more long-lived species (e.g., trees) the Δ^{14}C-signature is the average of the atmospheric CO_2 values (weighted by yearly carbon accumulation) over the plants' lifetime. Bottom-up estimation of $\Delta^{14}C_{bio}$ therefore requires information regarding the plant distribution in the area of interest, and the annual bioaccumulation of carbon for the different plants. As an alternative we here use the combined Δ^{14}C-signature of dissolved organic carbon (DOC) in three of the regions' major rivers, Congo, Zambezi and Tana, to obtain a regional $\Delta^{14}C_{bio}$ +57 ± 52 ‰, which is well in the expected range of a mixture of annual and multi-year plants (Marwick et al., 2015; Wild et al., 2019, Winiger et al., 2019).

The vegetation in SSA may be divided into two main classes: C_3-plants and C_4-plants – see discussion in Section 3.5. These two groups have distinct δ^{13}C-signatures, and may therefore be separated. We may then resolve three source classes by combining Δ^{14}C and δ^{13}C: C_3-plants, C_4-plants and fossil, through isotopic mass-balance (Andersson et al., 2015):

$$\begin{pmatrix} \Delta^{14}C \\ \delta^{13}C \\ 1 \end{pmatrix} = \begin{pmatrix} \Delta^{14}C_{C3} & \Delta^{14}C_{C4} & \Delta^{14}C_{fossil} \\ \delta^{13}C_{C3} & \delta^{13}C_{C4} & \delta^{13}C_{fossil} \\ 1 & 1 & 1 \end{pmatrix} \begin{pmatrix} f_{C3} \\ f_{C4} \\ f_{fossil} \end{pmatrix} \quad (2)$$

Endmember variability may significantly influence the calculated source fractional contributions (Andersson, 2011). For a discussion on the specific endmember ranges used here, see Section 3.5.

https://doi.org/10.5194/acp-2019-1027
Preprint. Discussion started: 19 November 2019

To account for the endmember variability, we implement a Bayesian approach, numerically resolve through Markov chain Monte Carlo simulations, implemented in Matlab, ver. 2015b (Andersson et al., 2015).

2.5 Remote Sensing and Air Mass Back trajectories.

Hourly 7-day air mass back trajectories (arrival height 2600 m.a.s.l.) were calculated using the NOAA Hybrid Single Particle Lagrangian Integrated Trajectory Model (HYSPLIT). Remote sensing fire-spot detections were retrieved from the NASA Fire Information for Resource Management Services (FIRMS) database, based on retrievals from the Moderate Resolution Imaging Spectroradiometer (MODIS) satellite product.

3 Results and Discussion

3.1 Rwanda and the monsoon

The meteorology of Rwanda is governed by the East African monsoon, with peak rainfalls in in April and November. There are thus two dry seasons, December-January-February (DJF) and the main dry season June-July-August (JAA). The dry periods in SSA are characterized by extensive biomass burning. During DJF the fires mainly occur to the north of Rwanda, and during JJA to the south (Fig. 1). Savannas are the main biomes in SSA, covering ~ 65% of the landmass, and are the main source of fire emissions (Cahoon et al., 1992). Located in a highly elevated region, Rwanda is, broadly speaking, surrounded by savanna regions, except to the west, where the tropical rainforests of Africa are located.

Air mass back trajectory analysis suggests that the air masses during the filter collection periods are overall easterly (Fig. 1). There is some overlap between the wet and JJA periods, but overall there is a seasonal switch, where the wet periods are more of northeastern origins (e.g., Kenya, Ethiopia and Somalia), whereas the dry JJA is more directly eastern/southeastern (e.g., Kenya, Tanzania). During JJA there are extensive fires to the south of RCO, mainly to the south-west. Given the easterly air mass transport, RCO is thus in general not directly downwind of these source regions. However, given the comparably low non-fire background emissions during this time, the

https://doi.org/10.5194/acp-2019-1027
Preprint. Discussion started: 19 November 2019

influence may still be significant; BT analysis is highly challenging in mountainous regions (e.g., Winiger et al., 2019), and the actual geographical footprints would be broader when, e.g., incorporating parametrizations for turbulence. Here we interpret the BTs qualitatively to visualize overall air mass transport patterns.

3.2 Concentrations of fine aerosol components

During the present campaign, the $PM_{2.5}$ carbonaceous and inorganic ion components show a strong seasonal variability, with elevated levels during the dry JJA period (Fig. 2, Table S1). The dry/wet period ratios for TC, EC, WSOC, NO_3^-, SO_4^{2-}, NH_4^+ and K^+, were 4.2, 7.0, 4.1, 12.6, 3.0, 3.2 and 8.8, respectively. This variability suggests differences in the aerosol regime, in addition to seasonality in meteorology, e.g., varying boundary layer heights or precipitation. The sea-salt contributions to the ions are overall estimated to be less than 1%, based on corrections with sodium ions (Blanchard and Woodcock, 1980). We here report the actual concentrations to ease direct comparisons with previous studies. Overall these differences reflect differences in aerosol atmospheric lifetime, differences in air mass transport pathways and seasonality in emissions (e.g., fires), as well as other factors. Elevated ratios of EC and K^+ suggests an increased influence from biomass burning during the dry season. NO_3^- - which displays the largest seasonal shift - is often associated with oxidized NO_x from traffic emissions or lightning strikes. However, it has also has also been shown to be elevated during savanna burning events (Table 1).

The dry season concentrations of the carbonaceous aerosols components and inorganic ions observed here are overall in good agreement with the concentrations observed dry season rural and aged savanna fire air masses (Table 1). The BC values are in the same range as has previously been observed at Mt. Kenya (0.72 ± 0.06 μgC m^{-3}, Gatari et al., 2003). During atmospheric aging of a biomass plume, the values of OC, EC and K^+ decrease by a factor of 2-3, whereas other components are ~ un-affected (Table 1). However, the effects appear variable, as compared with savanna fires in South Africa (Gao et al., 2003).

RCO is situated not far away from the downwind Nyiargongo and Nyamuragria Volcanoes in eastern Democratic Republic of Congo. Satellite-monitoring of the SO_2 emissions from these volcanos show a near-constant activity over the time period covering the present campaign,

https://doi.org/10.5194/acp-2019-1027
Preprint. Discussion started: 19 November 2019

potentially affecting the observed sulfate levels (Barrière et al., 2017). Here we observe an elevation in sulfate levels (~ 5µg m^{-3}) during the week starting of the 13th of June 2015 (Fig. 2), potentially indicating influence from volcanic emissions, but with no clear linkage to an increase in activity.

3.3 Source marker ratios and correlations

Overall, the ratios of different aerosol components provide insights into sources or atmospheric processes. Here, the OC/EC-ratio shows a distinct seasonality, with elevated levels during the wet season (11±3) compared to the dry season (7±3; Fig. 3; Table S1). The OC/EC-ratio is sometimes used as a marker for biomass burning, but it is highly influenced by atmospheric processes such as secondary organic aerosol (SOA) formation or photo-chemical aging (e.g., Dasari et al., 2019). The dry season values observed here are similar to what has been observed in background air at other dry season Sub-Saharan African sites (Table 1). The elevated wet-season OC/EC-ratios may indicate increased relative influence of local SOA formation.

Similarly, the NH_4^+/TC and SO_4^{2-}/TC are also elevated during the wet periods (Fig. 3), while decrease during the dry seasons, suggesting a different source profile compared to EC, K^+ and NO_3^-. In contrast, the WSOC/OC-ratio shows no clear seasonality, indicating that the sources and atmospheric processing of water-soluble and water-insoluble organic components are not changing significantly over the year. TC correlates with K^+ ($R^2 = 0.95$, $p<0.01$) and NO_3^- ($R^2 = 0.95$, $p<0.01$), suggesting that the incomplete combustion regime during the present campaign is governed by biomass burning emissions, e.g., savanna burning. Taken together, these ratios qualitatively suggest that the aerosol regime at RCO is strongly influenced by a pulse of biomass burning products during the JJA dry period.

3.4 Carbon isotopes

Radiocarbon ($\Delta^{14}C$) and stable-carbon ($\delta^{13}C$) provides detailed information regarding the sources and atmospheric processing of carbonaceous aerosols. Here, we investigated the signatures of TC for roughly every second sample during the campaign. The $\Delta^{14}C$-marker is not influenced by

https://doi.org/10.5194/acp-2019-1027
Preprint. Discussion started: 19 November 2019

atmospheric processing, and may be used to compute the relative contributions of fossil vs biomass/biogenic sources with high precision, Eq. (1). The $\Delta^{14}C$-signature show an oscillation over the seasons (Fig. 4), ranging between -84‰ (November, 2014) and +30‰ (July, 2015; Fig. 4; Table S1). Thus, during the JJA period, the $\Delta^{14}C$-signature occasionally exceed the signature for atmospheric CO_2 (+20‰, Graven, 2015; Turnbull, 2017).

Using Equation (1), the fraction biomass/biogenic TC for this sample is 97%. During the wet season, the fraction fossil reaches 13%, possibly of a more local character. $\Delta^{14}C$ correlates with 1/TC ($R^2 = 0.85$, $p<0.01$), suggesting a two-state source mixing regime between and background signal and a temporally varying source (Keeling, 1958, Fig. 4C). This inverse relation gives $\Delta^{14}C = +37 \pm 6$‰ as TC $\rightarrow \infty$, showing that the non-background state is dominated by biogenic/biomass burning emissions. The $\Delta^{14}C$-signatures for TC reported here are overall higher than what has been reported at receptor sites in South and East Asia (Sheesley et al., 2012; Kirillova et al., 2014; Bikkina et al., 2016).

In contrast to $\Delta^{14}C$, the $\delta^{13}C$-ratio is influenced by both atmospheric processes and atmospheric signatures. Here, the $\delta^{13}C$-ratio shows a similar pattern relative to the $\Delta^{14}C$-ratio, depleted (min -27‰) during wet periods, and enriched during JJA (max ~ -21 ‰). The $^{13}C/^{12}C$-ratio, has overall been found to be more enriched in aged air masses in South Asia, especially for WSOC (Sheesley et al., 2012; Kirillova et al., 2013). However, less so for TC. In fact, the enrichment of $\delta^{13}C$ in WSOC often appears to be counter-acted by the depletion in water-insoluble OC (e.g., Yan et al., 2017; Fang et al., 2017).

The TC $\delta^{13}C$ values, and their seasonal trend, are similar to what has previously observed in fine aerosols at a rural site in Tanzania (May – August, 2011, Mkoma, et al., 2014). However, the temporal trend appears shifted: for RCO from values around -25 ‰ to a ~ 22 ‰ around mid-May. At the Tanzanian site, a similar shift occurs in mid-June. In addition to the measurements being conducted at different sites during different years, there is a good agreement, and the temporal offset may be explained by ITCZ position variability. Similarly, the $\delta^{13}C$ for TC at savanna woodland site in Zambia, observed during August-September 2000, was -21.8±0.8 ‰ (Billmark et al., 2003), while values between -19.3 and –23.6 ‰ were observed at sites in the Ivory Coast (Cachier et al., 1985).

https://doi.org/10.5194/acp-2019-1027
Preprint. Discussion started: 19 November 2019

3.5. Carbon isotope-based source apportionment

By combining the $\Delta^{14}C$ and the $\delta^{13}C$-ratios we can by isotopic mass balance resolve three major sources of TC at the RCO. However, there are some important considerations to this approach: (1.) The $\delta^{13}C$-ratio is not an exclusive source marker, but is also affected by atmospheric processing (e.g., photo-chemical oxidation and secondary formation). (2.) The main source categories must be defined and distinguishable with carbon isotopes (3.) The source values of the isotope-signatures – the endmembers – and their natural variability need to be established.

As mentioned, the $\delta^{13}C$-ratio of bulk TC appears to be considerably less affected by atmospheric processing compared to sub-components, such as WSOC. Here, the temporal variation of the $\delta^{13}C$-ratio is qualitatively similar to that of $\Delta^{14}C$-ratio (Fig. 4). Since $\Delta^{14}C$ is not affected by atmospheric reactions, this suggests that source variability is a key driver of the $\delta^{13}C$ variability. Furthermore, the WSOC/OC is virtually constant throughout the year; the WSOC/OC-ratio has been found to be highly affected by atmospheric processing and related to shifting $\delta^{13}C$ (Kirillova et al., 2013; Yan et al., 2017; Fang et al., 2018; Dasari, 2019). Here, we therefore assume that the $\delta^{13}C$-ratio of TC is not strongly perturbed by atmospheric processing, and may thus be used as a source marker.

Turning to potential sources, there is a multitude of potential source categories for TC in SSA. However, many of these falls in broader categories, with similar carbon isotopic signatures. Around the world, the applications of dual carbon isotopes in ambient TC mainly identified/considered 6 broad source categories: C_3 plants, C_4 plants, liquid fossil (e.g., traffic), coal combustion (solid fossil), gas flaring (gaseous fossil) and marine emissions (Winiger et al., 2019; Andersson et al., 2015; Kirillova et al., 2013). Overall, the practice of coal combustion in SSA is expected to be much less frequent than in, e.g., South and East Asia, and we therefore do not consider this source further. In addition, marine emissions are not expected to have a large influence at RCO, supported by the low estimates of marine contributions to the inorganic ions (<1%). For gas flaring, there are potential distant sources around the Arabian Peninsula and off the west coast of Africa, in the Gulf of Guinea. However, given the distances to the RCO station and the prevailing wind directions, emissions from flaring are not expected to affect the site.

https://doi.org/10.5194/acp-2019-1027
Preprint. Discussion started: 19 November 2019

The remaining three main source categories are the two biomass sources of C_3 (e.g., trees) and C_4 plants (e.g., sugarcane and certain grasses) and liquid fossil. Aerosols from liquid fossil sources have a $\Delta^{14}C_{fossil}$ = -1000‰ (completely depleted in ^{14}C) and a $\delta^{13}C_{fossil}$ = -25.5±1.3‰ (Widory, 2006; Andersson et al., 2015). The $\Delta^{14}C$ of biomass was established in Section 2.4, and we set: $\Delta^{14}C_{C3} = \Delta^{14}C_{C4}$ = +57 ± 52‰. The $\delta^{13}C$ of C_3-plants in general is -27.1±2‰ (Bender, 1971; O'Leary, 1988). However, for aerosols generated from C_3-plants this value may be either enriched (e.g., ~ 0.5‰ biomass burning) or depleted (e.g., ~ 0 to 4‰ during SOA formation) (Turekian, 1998; Das et al. 2010, Mkoma et al., 2014; Aguilera and Whigham, 2018). In any case, the numerical spread in the $\delta^{13}C$ of these different scenarios are largely overlapping with that of the raw materials, and we therefore use this value here. The $\delta^{13}C$ of C_4-plants is -13.1±1.2‰ (Bender, 1971; O'Leary, 1988; Turekian 1998). During incomplete combustion, the $\delta^{13}C_{C4}$ may be depleted by a factor ranging between 0 to 7‰, largely dependent on burning conditions and different species (Martinelli, 2002; Das et al., 2010; Aguilera and Whigham, 2018). To account for these effects, we set $\delta^{13}C_{C4}$: -16.6 ± 2.2‰, where the standard deviation is propagated from the variability of the raw plant signature and one fourth of the maximum spread (7‰) of the depletion ($\sigma^2 = 1.2^2 + (7/4)^2$).

The fractional source contributions of fossil, C_3 and C_4 to TC may then be solved using these endmembers, using Eq. (2), (Fig. 5). It is well-established that accurate estimation of the fractional source contributions requires explicit incorporation of the endmember variability, and we here use a Bayesian framework driven by Markov chain Monte Carlo simulations for this purpose (Andersson, 2011; Andersson et al., 2015). The resulting fractional contributions display a large variability when comparing wet and dry conditions (Fig. 6A; Table S2). The dry season is characterized by relatively higher C_4-plant contributions, whereas the relative contributions of fossil and C_3-plants are higher during the wet periods. By combining the estimated fractional source contributions with the TC concentrations, we can estimate the concentrations from the different sources (Fig. 6B), revealing a more accentuated source variability. The average dry-to-wet ratios of the TC concentrations for C_3-plants, C_4-plants and fossil are 3, 4 and 2, respectively.

Savannas are the main biome for C_4-plants in SSA. For East African savannas, $\delta^{13}C$ data suggests that ~ 62% ($f_{C4,NPP}$) of the net primary production (NPP) is from C_4-plants (the rest mainly C_3-plants, Lloyd et al., 2008). Thus, one may assume that the source characteristics of TC emitted

https://doi.org/10.5194/acp-2019-1027
Preprint. Discussion started: 19 November 2019

from savanna burning should represent this plant-signature distribution. However, the aerosol emissions modulate the NPP activity by differences in emissions factors (EF). The uncertainties of EFs from different biomass burning activities are generally large and overlapping (Andreae, 2019). As a first approximation, we here use $f_{C4,NPP}$ to estimate the fractional contribution of savanna emissions to TC ($f_{savanna}$) as (i = sample index):

$$f_{savanna}(i) = \frac{f_{C4}(i)}{f_{C4,NPP}} \quad (3)$$

This analysis shows that the dry season carbonaceous aerosol regime is dominated by savanna fire emissions (Fig. 6), reaching up to 71%. These results agree with the elevated levels of EC, K^+ and NO_3^- during JJA.

5. Outlook

In this paper we find that that the aerosol regime of the emissions affecting the Rwanda Climate Observatory (RCO) may be described as a two-state source mixture: a regional/local background signal modulated by savanna fire emissions. Multiple studies have shown that savanna fires strongly influence the aerosol regime in SSA. Here, we quantify the savanna fire contributions for carbonaceous aerosols to range from 50% (wet period; $TC_{savanna}$ = 0.63 μg m^{-3}) to 71% (dry period; $TC_{savanna}$ = 9.7 μg m^{-3}) at a mountain background site in central SSA. The savanna fires are believed to be mainly lit by humans, and although these activities have been ongoing perhaps throughout the Holocene, these anthropogenic activities strongly perturb, e.g., the regional ecosystems, climate and air quality (e.g., Bird and Cali, 1998; Archibald et al., 1998). The annual SSA savanna carbon budget is a slight net CO_2 source to the atmosphere (Still et al., 2003; Williams, 2007; Cais et al., 2011; Valentini et al., 2014; Palmer et al., 2019). Finding more sustainable alternatives to the slash-and-burn practices in SSA may turn the region into a carbon sink. For instance, implementation of early dry season burning may be a possible strategy (Lipset-Moore et al., 2018). Savanna fire mitigation would also improve the regional air quality and stabilize precipitation patterns, but could also accelerate climate change by reducing cloud brightening (Hodnebrog et al., 2015; Lu et al., 2018; Heft-Neal et al., 2018; Bauer et al., 2019; Haslett et al., 2019).

https://doi.org/10.5194/acp-2019-1027
Preprint. Discussion started: 19 November 2019

Nevertheless, our current level of scientific understanding of the impact of savanna burning on the environmental system is poor, as are the couplings/responses to climate change, population growth, urbanization and other key socio-economic and environmental challenges for sustainable development in SSA (e.g., IPCC, 2014; Liousse et al., 2015; Brandt et al., 2017; UNDP, 2018). Savanna burning mitigation, or induced shifts due to, e.g., climate change, may change the present steady-state in unpredictable ways (e.g., Abreu et al., 2017). To better constrain the multiple environmental impacts of savanna burning in SSA, the comparably few ongoing ground-based in situ observations should be expanded and solidified (Williams, 2007; Cais et al., 2011; Kulmala, 2018; López-Ballesteros et a., 2018). For instance, observations of source-segregated aerosol concentrations provides multiple opportunities for advancing our knowledge base on SSA, including means for testing chemical-transport models; quantifying the relative importance of different atmospheric processes/emissions; assessing air quality effects; examining the relative importance of cooling vs warming (e.g., BC) aerosols; ground-truthing remote sensing products and detailed monitoring of the expected rapid change over the coming decades, including the effects of climate warming, population growth and urbanization.

Data availability: The chemical and isotopic data, as well as the MCMC-derived relative source contributions of C_3-plants, C_4-plants and fossil, and the corresponding source-segregated TC concentrations is provided in the supplementary information.

Competing interests: The authors declare that they have no conflict of interest.

Author contributions: AA wrote the manuscript, set-up the $PM_{2.5}$ high-volume sampler at RCO, and analyzed the data. ENK and SD conducted the carbonaceous aerosol quantifications and isolations for isotopes, and IC analysis. JG worked with the instruments, including helping or leading installation, and provided feedback on data analysis. KEP was instrumental in setting up the RCO and did most of the initial instrument installation. HLD served as the RCO station chief scientist for three years. JN and JdDN worked as technical coordinators of the project at different times and facilitated the operations of the station as well as providing feedback on analysis. BS

https://doi.org/10.5194/acp-2019-1027
Preprint. Discussion started: 19 November 2019

was our University of Rwanda liaison as the head of the Master's program in atmospheric and climate science. RGP is the head of the AGAGE network and is the MIT liaison to the RCO, and was essential in the setup of the observatory and scientific analysis. All authors commented on the manuscript.

Acknowledgements. We thank the generous MIT alumni donors to the MIT-Rwanda Climate Observatory Project that provided the funds to purchase, develop, and install most of the instruments at the Rwanda Climate Observatory. Additional funds for this purpose were provided by the MIT Center for Global Change Science. COMESA provided the funds to purchase and install the Aethalometer at the RCO. We also thank the Government of Rwanda and the Rwanda Ministry of Education, specifically Mike Hughes, Vianney Rugamba, and Marie Christine Gasingirwa, for supporting this project, including funding the staffing and infrastructure costs of the Rwanda Climate Observatory, and the University of Rwanda for providing laboratory space and infrastructure for instrument testing. We also wish to acknowledge the essential contributions of the Mugogo station technical experts Theobard Habineza, Modeste Mugabo, Olivier Shyaka, and Gaston Munyampundu and RBA technician Yves Fidele, without which running this station would be impossible. AA acknowledges project grants from the Swedish Research council (projects 348-2013-114 and 2017-05687). ENK acknowledges the People Programme (Marie Curie Actions) of the European Union's Seventh Framework Programme (FP7/2007-2013) under REA grant agreement 623386. We acknowledge the use of data and imagery from LANCE FIRMS operated by NASA's Earth Science Data and Information System (ESDIS) with funding provided by NASA Headquarters. The authors gratefully acknowledge the NOAA Air Resources Laboratory (ARL) for the provision of the HYSPLIT transport and dispersion model and/or READY website (http://www.ready.noaa.gov) used in this publication.

https://doi.org/10.5194/acp-2019-1027
Preprint. Discussion started: 19 November 2019

References

Abreu, R.C., Hoffmann, W.A., Vasconcelos, H.L., Pilo, N.A., Rossatto, D.R., Durigan, G.: The biodiversity cost of carbon sequestration in tropical savanna. Sci. Advan. 3, doi: 10.1126/sciadv.1701284, 2017.

Aguilera, J., Whigham, L.D.: Using the $^{13}C/^{12}C$ carbon isotope ratio to characterize the emission sources of airborne particulate matter: a review of literature. Isotopes Environ. Health. Stud 54, 573-587, doi: 10.1080/10256016.2018.1531854, 2018.

Andersson, A.: A systematic examination of a random sampling strategy for source apportionment calculations. Sci. Tot. Environ. 412-413, 232-238, doi: 10.1016/j.scitotenv.2011.031, 2011.

Andersson, A., Deng, J., Du, K., Zheng, M., Yan, C., Sköld, M., Gustafsson, Ö.: Regionally-varying combustion sources of the January 2013 severe haze events over Eastern China. Environ. Sci. Technol. 49, 2038-2043, doi: 10.1021/es503855e, 2015.

Andreae, M.O.: Emission of trace gases and aerosols from biomass burning – An updated assessment. Atmos. Chem. Phys. Discuss. doi: 10.5194/acp-2019-303, 2019.

Archibald, S., Staver, A.C., Levin, S.A.: Evolution of human-driven fire regimes in Africa. Proc. Nat. Acad. Sci. 109, 847-852, doi: 10.1073/pnas.1118648109, 2012.

Aurela, M., Beukes, J.P., van Zyl, P., Vakkari, V., Teinilä, K., Saarikoski, S., Laakso, L.: The composition of ambient and fresh biomass: burning aerosols at a savannah site, South Africa. South Afr. J. Sci. 112, 1-8, doi: 10.17159/ sajs.2016/20150223, 2016.

Barrière, J., Oth, A., Theys, N., d'Oreye, N., Kervyn, F.: Long-term monitoring of long-period seismicity and space-based SO_2 observation at African lava lake volcanoes Nyiarango and Nyamulagira (DR Congo). Grophys. Res. Let. 44, 6020-6029, doi: 10.1002/2017GL073348, 2017.

Bauer, S.E., Im, U., Mezuman, K., Gao, C.Y.: Desert dust, industrialization, and agricultural fires: health impacts of outdoor air pollution in Africa. J. Geophys. Res. 124, 4104-4120, doi: 10.1029/2018JD029336, 2019.

Bender, M.M.: Variations in the $^{13}C/^{12}C$ ratios of plants in relation to the pathway of photosynthetic carbon dioxide fixation. Phytochem. 10, 1239-1244, doi: 10.1016.S0031-9422(00)84324-1, 1971.

Bikkina, S., Andersson, A., Sarin, M.M., Sheesley, R.J., Kirillova, E., Rengarajan, R., Sudheer, A.K., Ram, K., Gustafsson, Ö.: Dual isotope characterization of total organic carbon in wintertime carbonaceous aerosols for northern India. J. Geophys. Res. 121, doi: 10.1002/2016JD024880, 2016.

Billmark, K.A., Swap, R.A., Macko, S.A.: Stable isotope and GC/MS characterization African aerosols. South African J. Sci. 101, 177-170, 2005.

Birch, M.E., Cary, R.A.: Elemental carbon-based method for monitoring occupational exposures to particulate diesel exhaust. Aerosol Sci. Technol 25, doi: 10.1080/02786829608965393, 1996.

Bird, M.I., Cali, J.A.: A million-year record of fire in sub-Saharan Africa. Nature 394, 767-769, doi: 10.1038/29507, 1998.

Blanchard, D.C., Woodcock, A. H.: The production, concentration, and vertical distribution of the sea-salt aerosol. Annal. N.Y. Acad. Sci. doi: 10.1111/j.1749-6632.1980.tb17130.x, 1980.

Bond, T.C., Doherty, S.J., Fahey, D.W., Forster, P.M., Berntsen, T., DeAngelo, B.J., Flanner, M.G., Ghan, S., Kärcher, B., Koch, D., Kinne, S., Kondo, Y., Quinn, P.K., Sarofim, M.C., Schultz, M.G., Schultz, M., Venkataram, C., Zhang, H., Zhang, S., Bellouin, N., Guttikunda, S.K., Hopke, P.K., Jacbonson, M.Z., Kaiser, J.W., Klimont, Z., Lohmann, U., Schwarz, J.P., Shindell, D., Storelvmo, T., Warren, S.G., Zender, C.S.: Bounding the role of black carbon in the climate system: A systematic assessment. J. Geophys. Res. 118, 5380-5552, doi: 10.1002./jgrd.50171, 2013.

Brandt, M., Rasmussen, K., Penuelas, Tian, F., J., Schurgers, G., Verger, A., Mertz, O., Palerm, J.R.B., Fensholt, R.: Human population growth offsets climate-driven increase in woody vegetation in sub-Saharan Africa. Nature Ecol. Evol. 1, doi: 10.1038/s41559-017-0081, 2017.

Brito, J., Freney, E., Dominutti, P., Borbon, A., Haslett, S.L., Batenburg, A.M., Colomb, A., Dupuy, R., Denjean, C., Burnet, F., Bourriane, T., Deroubaix, A., Sellegri, K., Borrmann, S. Coe,

H., Flamant, C., Knippertz, P., Schwarzenboeck, A.: Assessing the role of anthropogenic and biogenic source on PM1 over southern West Africa using aircraft measurements. Atmos. Chem. Phys. 18, 757-772, doi: 10.5194/acp-18-757-2018, 2018.

Cachier, H., Buat-Menard, P., Fontuge, M., Ranhcer, J.: Source terms and source strengths of the carbonaceous aerosol in the tropics. J. Atmos. Chem. 3, 469-489, doi: 10.1007/BF00053872, 1985.

Cahoon, D.R., Stocks, B.J., Levine, J.S., Cofer III, W.R., O'Neil, K.P.: Seasonal distribution of African savanna fires. Nature, 359, 812-815, doi: 10.1038/359812a0 , 1992.

Cais, P., Bombelli, A., Williams, M., Piao, S.L., Chave, J., Ryan, C.M., Henry, M., Brender, P., Valentini, R.: The carbon balance of Africa: synthesis of recent research studies. Phil. Trans. Roy. Soc. A 369, 2038-2057, doi: 10.1098/rsta.2010.0328, 2011.

Das, O., Wang, Y., Hsieh, Y.-P.: Chemical and carbon isotopic characteristics of ash and smoke derived from burning of C3 and C4 grasses. Org. Geochem. 41, 263-269, 10.1016/j.orggeochem.2009.11.001, 2010.

Dasari, S., Andersson, A., Bikkina, S., Holmstrand, H., Budhavant, K., Sateesh, S., Asmi, E., Kesti, J., Backman, J., Salam, A., Singh Bisht, D., Tiwari, S., Hameed, S., Gustafsson, Ö.: Photochemical degradation affects the light absorption of water-soluble brown carbon in the South Asian outflow. Sci. Adv. 5, doi: 10.1126/sciadv.aau8066, 2019.

DeWitt, H.L., Gasore, J., Rupakheti, M., Potter, K.E., Prinn, R.G., Ndikubwimana, JdD., Nkusi, J., Safari, B.: Seasonal and diurnal variability in O3, black carbon, and CO measured at the Rwanda Climate Observatory. Atmos. Chem. Phys, 19, 2063-2078, doi: 10.5194/acp-19-2063-201, 2019.

Fang, W., Andersson, A., Zheng, M., Lee, M., Holmstrand, H., Kim, S-W., Du, K., Gustafsson, Ö.: Divergent evolution of carbonaceous aerosols during dispersal of East Asian haze. Sc. Rep. 7, doi: 10.1038/s41598-017-10766-4, 2017.

Formenti, P., Elbert, W., Maenhaut, W., Haywood, J., Osborne, S., Andreae, M.O.: Inorganic and carbonaceous aerosols during the Southern African Regional Science Initiative (SAFARI 2000)

experiment: Chemical characteristics, physical properties, and emission data for smoke from African biomass burning. J. Geophys. Res. 108. Doie: 10.1029/2002JD002408, 2003.

Gao, S., Hegg, D.A., Hobbs, P.V., Kirchstetter, T.W., Magi, B.I., Sadilek, M.: Water-soluble organic components in aerosols associated with savanna fires in southern Africa: Identification, evolution and distribution. J. Geophys. Res. 108, doi: 10.1029/2002JD002324, 2003.

Gatari, M.J., Boman, J.: Black carbon and total carbon measurements at urban and ruralt sites in Kenya, East Africa. Atmos. Environ. 8, 1149-1154, doi: 10.1016/S1352-2310(02)01001-4, 2003.

Graven, H.: Impact of fossil fuel emissions on atmospheric radiocarbon and various applications of radiocarbon over this century. Proc. Nat. Acad. Sci. 112, 9542-9545, doi: 10.1073/pnas.1504467112, 2015.

Gustafsson, Ö., Kruså, M., Zencak, Z., Sheesley, R.J., Granat, L., Engström, E., Praveen, P.S., Rao, P.S.P., Leck, C., Rodhe, H.: Brown clouds over South Asia: Biomass or fossil fuel combustion? Science 323, 495-498, doi: 10.1126/science.1164857, 2009.

Haslett, S.L., Taylor, J.W:, Evans, M., Morris, E., Vogel, B., Dajuma, A., Brito, J., Batenburg, A.M., Borrmann, S., Schneider, J., Schulz, C., Denjean, C., Bourrianne, T., Knippertz, P., Dupuy, R., Schwarzenböck, A., Sauer, D., Flamant, C., Dorsey, J., Crawford, J., Coe, H.: Remote biomass burning dominates southern West African air pollution during the monsoon, Atmos. Chem. Phys. Discuss. doi: 10.5194/acp-2019-38, 2019.

Heft-Neal, S., Burney, J., Bendavid, E., Burke, M.: Robust relationship between air quality and infant mortality in Africa. Nature 559, 254-258, doi: 10.1038/s41586-018-0263-3, 2018.

Hodnebrog, Ø., Myhre, G., Forster, P.M., Sillman, J., Samset, B.H.: Local biomass burning is a dominant cause of the observed precipitation reduction in southern Africa. Nature Com. 7, doi: 10.1038/ncomms11236, 2015.

IPCC – Inter-Governmental Panel for Climate Change: AR5 Climate Change 2013: The physical science basis. ISBN 978-1107661820, 2013.

IPCC – Inter-Governmental Panel for Climate Change: AR5 Climate Change 2014: Impacts, adaptation and vulnerability. ISBN 978-1-107-68386-0, 2014.

Keeling, C.D.: The concentration and isotopic abundances of atmospheric carbon dioxide in rural areas. Geochem. Cosmochim. Acta. 13, 322-334, doi: 10.1016/0016-7037(58)90033-4, 1958.

Kirchstetter, T.W., Novakov, T., Hobbes, P.V., Magi, B.: Airborne measurements of carbonaceous aerosols in southern Africa during the dry biomass season. J. Geophys. Res. 108. Doi: 10.1029/2002JD002171, 2003.

Kirillova, E.N., Andersson, A., Sheesley, R.J., Kruså, M., Praveen, P.S., Budhavant, K., Safai, P.D., Rao, P.S.P., Gustafsson Ö: ^{13}C and ^{14}C-based study of sources and atmospheric processing of water-soluble organic carbon (WSOC) in South Asian aerosols. J. Geophys. Res. 118, 621-626, doi: 10.1002/jgrd.50130, 2013.

Kirillova, E.N., Andersson, A., Han, J., Lee, M., Gustafsson, Ö.: Sources and light absorption of water-soluble organic carbon aerosols in the outflow from northern China. Atmos. Chem. Phys. 14, 1413-1422, doi: 10.5194/acp-14-1413-2014, 2014.

Kulmala, M.: Build a global Earth Observatory. Nature 553, 21-23, 2018.

Liousse, C., Assamoi, E., Criqui, C., Rosset, R.: Explosive growth in African combustion emissions from 2005 to 2030. Environ. Res. Lett. 9, doi: 10.1088/1748-9326/9/3/035003, 2014.

Lipset-Moore, G.J., Wolff, N., Game, E.T.: Emissions mitigation opportunities for savanna countries from early dry season fire management. Nature Com. 9, doi: 10.1038/s41467-018-04687-7, 2018.

Lloyd, J., Bird, M.I., Vellen, L., Miranda, A.C., Veenendaal, E.M., Djagbletey, G., Miranda, H.S., Cook, G., Faruqhar, G.D.: Contributions of woody and herbacoues vegetation to tropical savanna ecosystem productivity: a quasi-global estimate. Tree Phys. 28, 451-468, doi: 10.1093/treephys/28.3.45, 2008.

López-Ballesteros, A:, Beck, J., Bombelli, A., Grieco, E., Lorenkova, E.K., Merbold, L., Brümmer, C:, Hugo, W., Scholes, R., Vackar, D., Vermeulen, A., Acosta, M., Butterbach-Bahl, K., Helmschrot, J., Kim, D.-G., Jones, M., Jorch, V., Pavleka, M., Skjelvan,I., Saunders, M.: Towards a feasible and representative pan-African research infrastructure network for GHG observations. Environ. Res. Lett. 13, doi: 10.1088/1748-9326/aad66c, 2018.

Lu, Z., Liu, X., Zhao, C., Meyer, K., Rajapakshe, C., Wu, C., Yang, Z., Penner, J.E.: Biomass smoke from southern Africa can significantly enhance the brightness of stratocumulus over the southeastern Atlantic Ocean. Proc. Nat. Acad. Sci, 115, 2924-2929, doi: 10.1073/pnas.1713703115, 2018.

Maenhaut, W., Salma, I., Cafmeyer, J., Annegarn, H.J., Andreae, M.O.: Regional atmospheric aerosols composition and sources in the eastern Transvaal, South Africa, and impact of biomass burning. J. Geophys. Res. 101, 23631-23650, 1996.

Martinelli, L.A., Camargo, P.B., Lara, L.B.L.S., Victoria, R.L., Artaxo, P.: Stable carbon and nitrogen isotopic composition of bulk aerosol particles in a C4 plant landscape of southeast Brazil. Atmos. Environ. 36, 2427-2432, doi: 10.1016/S1352-2310(01)00454-X, 2002.

Marwick, T.R., Tamooh, F., Teofuru, C.R., Borget, A.V:, Darchambeau, F., Bouillon, S.: The age of river-transported carbon: global perspective. Glob. Biogeochem. Cyc. 29, 122-137, doi: 10.1002/2014GB004911, 2015.

Mkoma, S.L., Kawamura, K., Tachibana, E., Fu, P.: Stable carbon and nitrogen isotopic compositions of tropical atmospheric aerosols: sources and contribution from burning of C_3 and C_4 plants to organic aerosols. Tellus B, 66, 1-12, doi: 10.3402/tellusb.v66.20176, 2014.¨

O'Leary, M.H.: Carbon isotopes in photosynthesis. Bioscience 38, 328–36, doi: 10.2307/1310735, 1988.

Palmer, P.I., Feng, L., Chevallier, F., Bösch, H., Somkuti, P.: Net carbon emissions from African biosphere dominate pan-tropical atmospheric CO_2 signal. Nature Com. 10. doi: 10.1038/s41467-019-11097-w, 2019.

Puxbaum, H., Rendl, J., Allabashi, R., Otter, L., Scholes, M.C.: Mass balance of the atmospheric aerosol in a South African savanna (Nylsvley, May 1997). J. Geophys. Res. 105, 20697-20706, 2000.

Sheesley, R.J., Kirllova, E.N., Andersson, A., Kruså, M., Praveen, P.S., Budhavant, K., Safai, P.D., Rao, P.S.P., Gustafsson, Ö.: Year-round radiocarbon-based source apportionment of carbonaceous

aerosols at two background sites in South Asia. J. Geophys. Res. 117, doi: 10.1029/2011JD017161, 2012.

Sinha, P., Hobbs, P.V., Yokelson, R.J., Bertschi, I.T., Blake, D.R., Simpson, I.J., Gao, S., Kirchstetter, T.W., Novakov, T.: Emissions of trace gases and particles from savanna fires in southern Africa. J. Geophys. Res. 108, doi: 10.1029/2002JD002325, 2003.

Still, C.J., Berry, J.A., Collatz, G.J., DeFries, R.S.: Global distribution of C_3 and C_4 vegetation: Carbon cycle implications. Glob. Biogeochem. Cyc. 17, doi: 10.1029/200GB001807, 2003.

Swap, R.J., Annegard, H.J., Suttles, J.T., King, M.D., Platnick, S., Privette, J.L., Scholes, R.J.: Africa burning: A thematic analysis of the Southern African regional science initiative (SAFARI 2000). J. Geophys. Res. 108, doi: 10.1029/2003JD003747, 2003.

Tiitta, P., Vakkari, V., Croteau, P., Beukes, J.P., van Zyl, P.G., Josipovic, M., Venter, A.D., Jaaros, K., Pienaar, J.J., Ng, N.L., Canagaratna, M.R:, Jayne, J.T., Kerminen, V.-K., Kokola, H., Kulmala, M., Laaksonen, A., Worsnop, D.R., Laakso, L.: Chemical composition, main sources and temporal variability of PM1 aerosols in southern African grassland. Atmos. Chem. Phys. 14, 1909-1927, doi: 10.5194/acp-14-1909-2014, 2014.

Turekian, V. C., Macko, S., Swap, R. J. and Garstang, M.: Causes of bulk carbon and nitrogen isotopic fractionations in the products of vegetation burns: laboratory studies. Chem. Geol. 152, 181-192, 10.1016/S0009-2541(98)00105-3, 1998.

Turnbull, J.C., Mikaloff Fletcher, S.E., Ansell, I., Brailsford, G.W., Moss, R.C., Norris, M.W., Steinkamp, K.: Sixty years of radiocarbon dioxide measurements at Wellington, New Zealand: 1965-2014. Atmos. Chem. Phys. 17, 14771-14784, doi: 10.5194/acp-17-14771-2017, 2017.

UNDP – United Nations Development Programme: 2018 Africa Sustainable Development Report: Towards a transformed and resilient continent. ISBN: 978-92-1-125134-0, 2018.

UNEP/WMO – United Nations Environment Programme/World Meteorological Organization: Integrated assessment of black carbon and tropospheric ozone. ISBN: 978-92-807-3142-2, 2012.

https://doi.org/10.5194/acp-2019-1027
Preprint. Discussion started: 19 November 2019

Valentini, R., Arneth, A., Bombelli, A., Castaldi, S., Cazzolla Gatti, R., Chevallier, F., Cias, P., Grieco, E., Hartmann, J., Henry, M., Houghton, R.A., Jung, M., Kutsch, W.L., Malhi, Y., Mayorga, E., Merbold, L., Murray-Tortarolo, G., Papale, D., Peylin, P., Poulter, B:, Raymond, P.A., Santini, M., Sitch, S., Vaglio Laurin, G., van der Werf, G.R., Williams, C.A., Scholes, R.J.: A full greenhouse gases budget of Africa: synthesis, uncertainties, and vulnerabilities. Biogeosciences 11, 381-407, doi: 10.5194/bg-11-381-2014, 2014.

WHO – World Health Organization: Health effects of black carbon. ISBN: 978 92 890 0265 3, 2012.

WHO – World Health Organization: Ambient air pollution: A global assessment of exposure and burden of disease. ISBN: 9789241511353, 2016.

Widory, D.: Combustibles, fuels and their combustion products: A view through carbon isotopes. Combust. Theory Mod. 10, 831-841, doi: 10.1080/13647830600720264, 2006.

Wild, B., Andersson, A., Bröder, L., Vonk, J:, Hugelius, G., McClelland, J.W., Song, W., Raymond, P.A., Gustafsson, Ö.: Rivers across the Siberian Arctic unearth the patterns of carbon release from thawing permafrost. Proc. Nat. Acad. 116, 10280-10285, doi: 10.1073/pnas.181179116, 2019.

Williams, C.A., Hanan, N.P., Neff, J.C., Scholes, R.J., Berry, J.A., Denning, S.A., Baker, D.F.: Africa and the global carbon cycle. Carbon Bal. Manag. 2, 1-13, doi: 10.1186/1750-0680-2-3, 2007.

Winiger, P., Barrett, T.E., Sheesley, R.J:, Huang, L., Sharma, S., Barrie, L.A., Yttri, K.E., Evangeliou, N., Eckhardt, S., Stohl, A., Klimont, Z., Heyes, C., Semiletov, I.P., Dudarev, O.V., Charkin, A., Shakhova, N., Holmstrand, H., Andersson, A., Gustafsson, Ö.: Source apportionment of circum-Arctic atmospheric black carbon from isotopes and modelling. Sci. Adv. 5, doi: 10.1126/sciadv.aau8052, 2019.

https://doi.org/10.5194/acp-2019-1027
Preprint. Discussion started: 19 November 2019

Yan, C., Zheng, M., Bosch, C., Andersson, A., Desyaterik, Y., Sullivan, A.P., Collett, J.L., Zhao, B., Wang, S., He, K., Gustafsson, Ö.: Important fossil source contribution to brown carbon in Beijing during Winter. Sci. Rep. 7, doi: 10.1038/srep43182, 2017.

https://doi.org/10.5194/acp-2019-1027
Preprint. Discussion started: 19 November 2019

TABLES

Table 1. Concentrations (μg m^{-3}; μgC m^{-3} for carbonaceous components) of fine aerosol components from ground-based and airborne measurements over Sub-Saharan Africa (bkg = background).

Sampling site	TC	OC	BC/EC	WSOC	NO_3^-	SO_4^{2-}	NH_4^+	K^+
RCO, dry[a]	9.5±3.7	8.2±3.2	1.3±0.6	5.7±2.1	1.2±0.7	2.1±1.0	0.8±0.3	0.7±0.3
RCO, wet[a]	2.4±1.2	2.2±1.1	0.20±0.1	1.5±0.7	0.1±0.1	0.7±0.3	0.3±0.1	0.08±0.05
Rural Tanzania, dry[b]	7±2	6±2	1.0±0.3	4±1	0.18±0.06	0.2±0.1	0.9±0.7	1.5±0.7
Rural Tanzania, wet[b]	4±1	4±1	0.5±1.3	3±1	0.06±0.03	0.1±0.1	0.2±0.1	0.4±0.2
Aircraft, Southern Africa, smoke[c]	N/A	N/A	N/A	N/A	4.84±0.02	10.4±0.6	N/A	13.1±0.1
Aircraft, Southern Africa, bkg[c]	N/A	N/A	N/A	N/A	0.48±0.00	2.2±0.1	N/A	0.31±0.02
Aircraft, Southern Africa fresh[d]	N/A	20±18	2±1	N/A	1.4±1.8	1.9±1.4	1.6±2.4	4.5±8.1
Aircraft, Southern Africa aged[d]	N/A	6±3	1.03±0.04	N/A	1.0±0.8	2.0±1.5	0.9±0.8	0.6±0.4
Aircraft, Southern Africa, plume[e]	106±86	91±74	15±12	N/A	N/A	N/A	N/A	N/A
Aircraft, Southern Africa haze[e]	10.5±8.2	9.5±6.8	2.3±1.8	N/A	N/A	N/A	N/A	N/A
Aircraft, Southern Africa[f]	8.5±4.8	N/A	2.3±1.9	N/A	0.8±0.3	4.5±3.6	N/A	0.4±0.1
National Park, South Africa[g]	N/A	N/A	1.2 - 2.2	N/A	N/A	N/A	N/A	0.22 - 0.34
Savanna, South Africa[h]	9.1	N/A	0.61	N/A	0.4	11.08	2.85	0.28
Aircraft, W. Africa, bkg[i]	N/A	N/A	0.33 – 0.35	N/A	0.11 – 0.12	1.64 – 1.70	0.63 – 0.68	N/A
Aircraft, W. Africa, urban plume[i]	N/A	N/A	0.64 – 0.72	N/A	0.49 – 0.53	2.70 – 3.03	1.20 – 1.38	N/A
Grassland, South Africa, dry[j]	N/A	N/A	0.6	N/A	0.3	1.4	0.2	N/A
Grassland, South Africa, wet[j]	N/A	N/A	0.3	N/A	0.2	0.4	0.3	N/A
Savanna, South Africa, spring[k]	N/A	N/A	0.40	N/A	0.05	2.48	0.05	0.17
Savanna, South Africa, summer[k]	N/A	N/A	0.16	N/A	0.01	5.65	0.01	0.2

a. Present study
b. Mkoma et al., 2014
c. Gao et al., 2003
d. Formenti et al., 2003
e. Kirchstetter et al, 2003
f. Sinha et al., 2003
g. Maenhaut et al., 1996
h. Puxbaum et al., 2000
i. Brito et al., 2018
j. Tiitta et al., 2014
k. Aurela et al., 2016

https://doi.org/10.5194/acp-2019-1027
Preprint. Discussion started: 19 November 2019

FIGURES

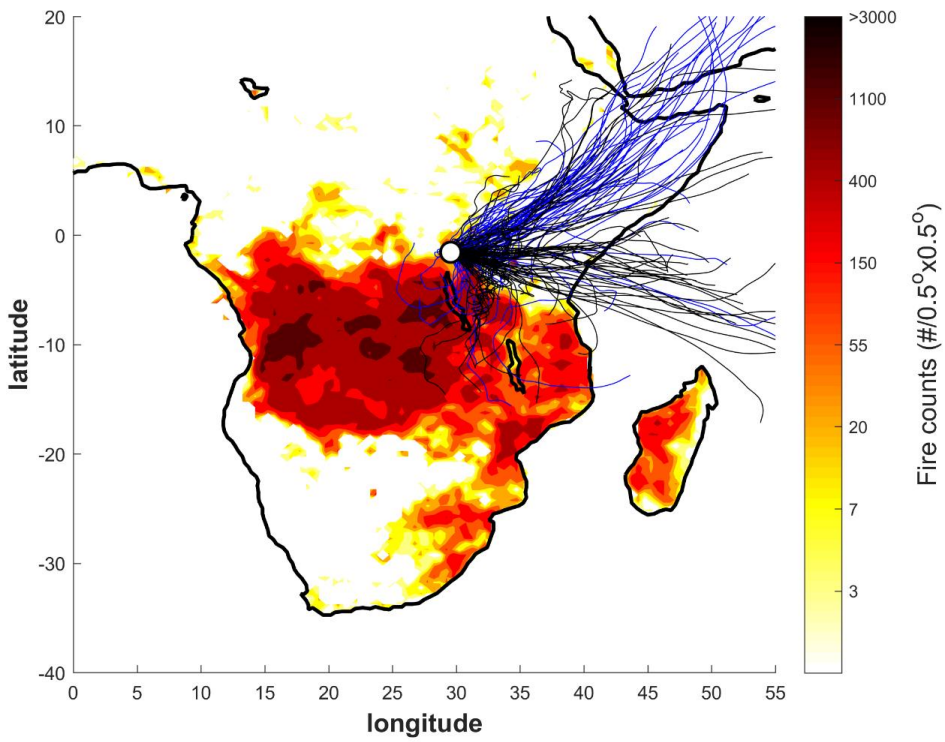

Figure 1. Fire counts and air mass back trajectories for the October 2014 to September 2015 campaign at the Rwanda Climate Observatory (RCO, black and white circle). The fire counts are from the Fire Information for Resource Management System (FIRMS) derived from the NASA Moderate Resolution Imaging Spectroradiometer (MODIS) satellite product for June-July-August (JJA), 2015. The thin lines represent daily (3AM, C.A.T.) 7-day air mass back-trajectories arriving at RCO. The blue lines correspond to what we here refer to the 'wet' period (October-November 2014 and April-May 2015), whereas the black lines represent the dry JJA period.

https://doi.org/10.5194/acp-2019-1027
Preprint. Discussion started: 19 November 2019

Atmospheric Chemistry and Physics Discussions

Figure 2. Concentrations of carbonaceous aerosols (TC = total carbon; EC = elemental carbon; OC = organic carbon; WSOC = water-soluble organic carbon) and inorganic ions in $PM_{2.5}$ during October 2014 to September 2015 at the Rwanda Climate Observatory. The November 2014 to April 2015 gap is due to a lightning strike. The concentrations of EC were multiplied by 5 and K^+ by 2 for visual clarity.

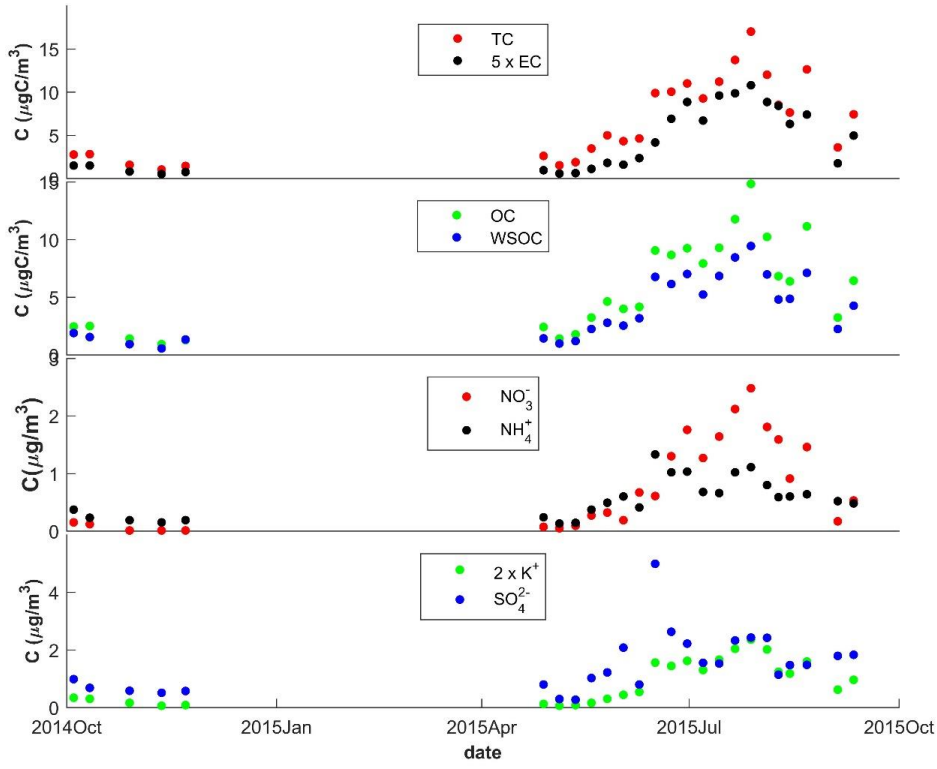

https://doi.org/10.5194/acp-2019-1027
Preprint. Discussion started: 19 November 2019

Figure 3. Ratios of carbonaceous aerosols (EC = elemental carbon; OC = organic carbon; WSOC = water-soluble organic carbon) and inorganic ions relative to total carbon (TC) in $PM_{2.5}$ during October 2014 to September 2015 at the Rwanda Climate Observatory. The November 2014 to April 2015 gap is due to a lightning strike. The concentrations of K^+/TC and NH_4^+/TC ratios were multiplied by 2 for visual clarity.

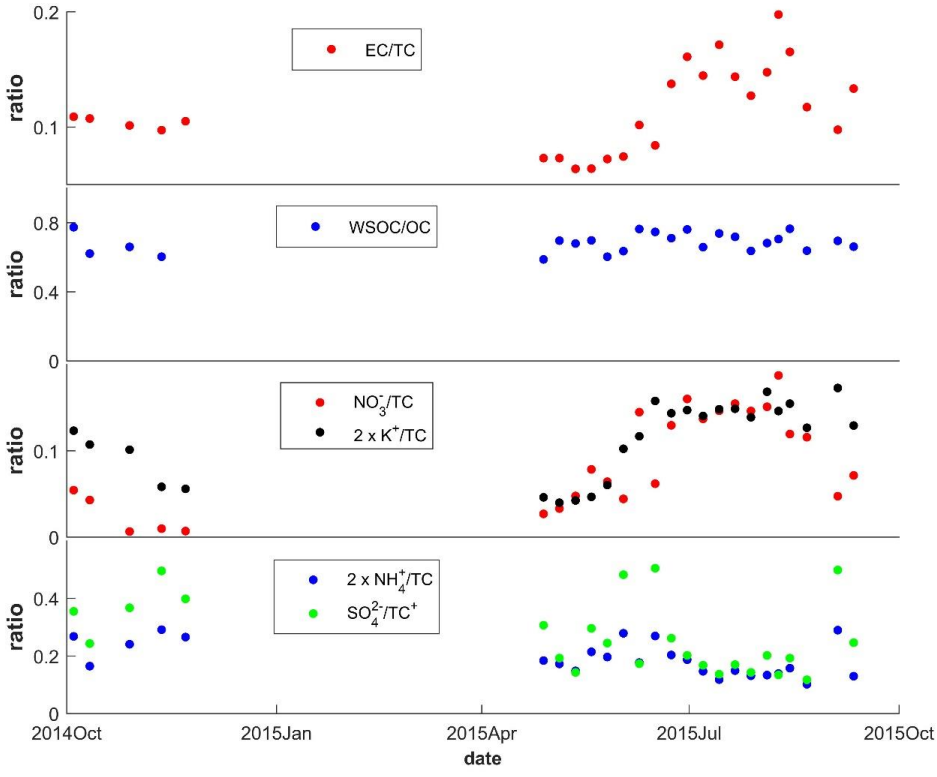

https://doi.org/10.5194/acp-2019-1027
Preprint. Discussion started: 19 November 2019

Figure 4: Dual carbon isotope data for TC. Panel A. $\Delta^{14}C$ vs time. Panel B. $\delta^{13}C$ vs time. Panel C. $\Delta^{14}C$ vs TC (blue circles). The black line is the fit of the equation $\Delta^{14}C = A/[TC]+B$, using Markov chain Monte Carlo simulations, where A and B are fitting parameters (A= -135±16 ‰ μg m^{-3}; B= 37±6 ‰). The grey shaded area is the 1σ spread of the fit.

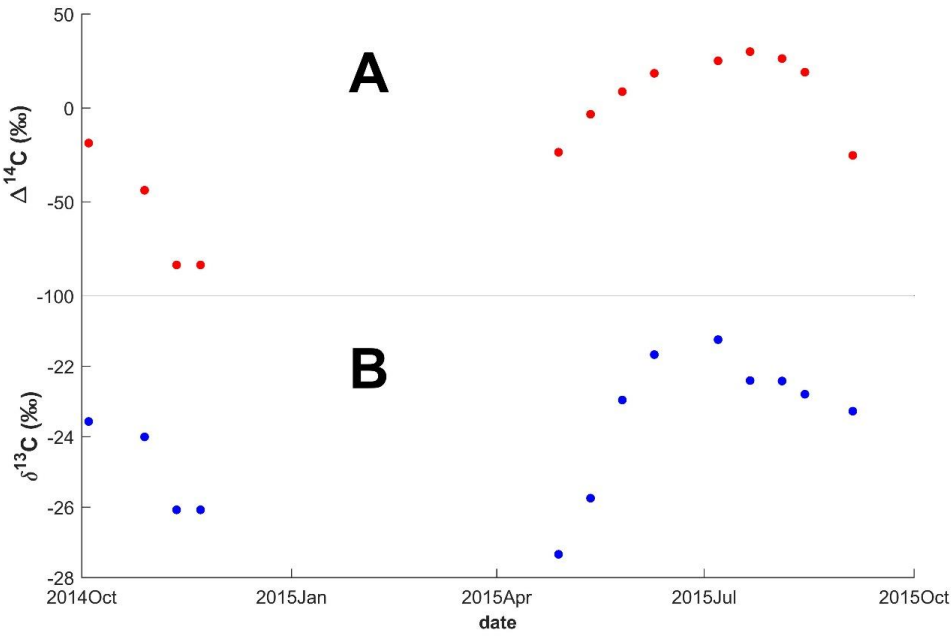

https://doi.org/10.5194/acp-2019-1027
Preprint. Discussion started: 19 November 2019

Atmospheric Chemistry and Physics
Discussions

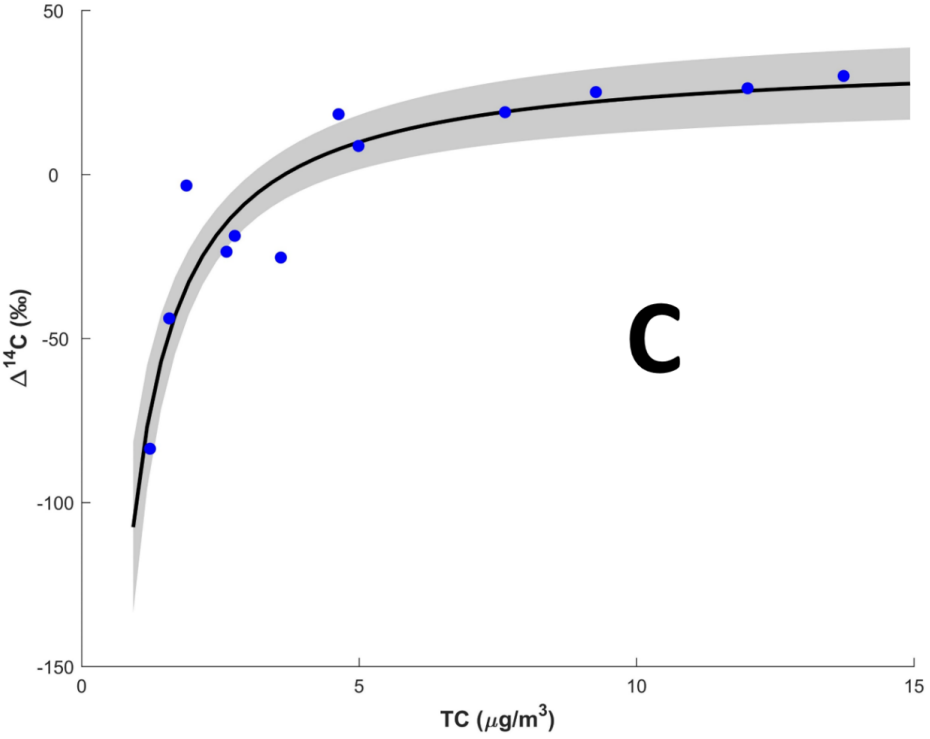

683

https://doi.org/10.5194/acp-2019-1027
Preprint. Discussion started: 19 November 2019

Figure 5: Dual carbon ($\Delta^{14}C$ vs $\delta^{13}C$) isotope plot of TC. Blue circles represent Oct-Nov 2014 (wet), yellow circles Apr-May 2015 (wet), and red circles Jun-Sept 2015 (dry). The boxes represent the endmember ranges (mean ± stdev; see Section 3.5) of the three main sources: C_3-plants (green), C_4-plants (orange), and fossil (black).

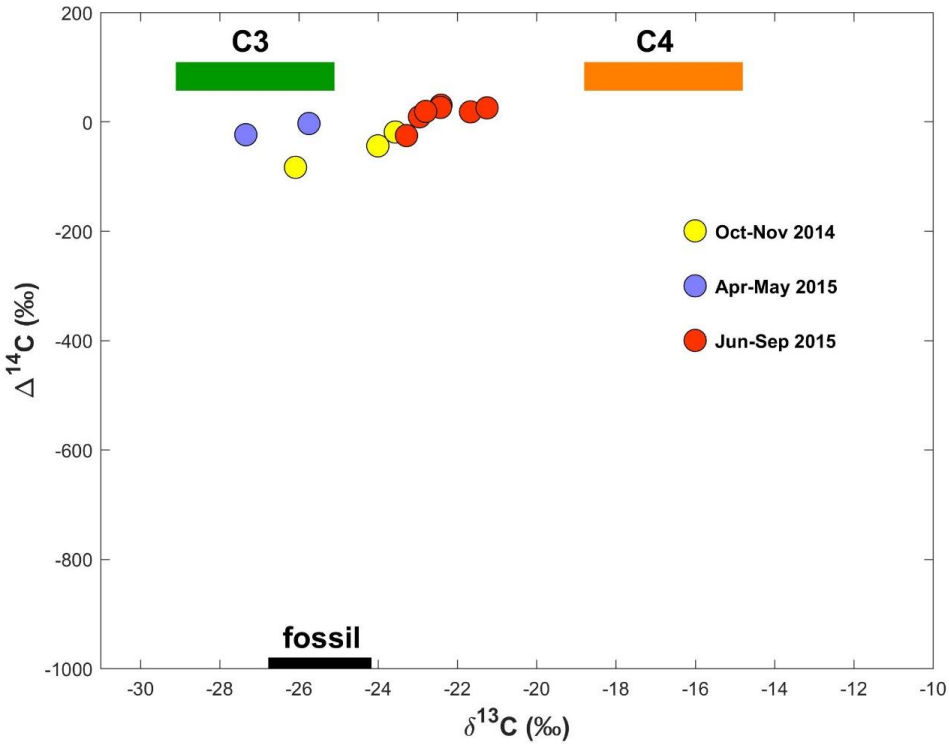

https://doi.org/10.5194/acp-2019-1027
Preprint. Discussion started: 19 November 2019

Figure 6: Carbon isotope-source segregated fractions and concentrations of TC vs time. Panel A. Relative source contributions (%) of C_3-plants (green circles), C_4-plants (orange diamonds) and fossil (black triangles). The error bars (standard deviations) were constrained using Markov chain Monte Carlo simulations. Panel B. Source segregated concentrations of TC of C_3-plants (green circles), C_4-plants (orange diamonds) and fossil (black triangles).